

CNN-LSTM and Transfer Learning Models for Malware Classification based on Opcodes and API Calls

Ahmed Bensaoud^{a,*}, Jugal Kalita^a

^aDepartment of Computer Science, University of Colorado Colorado Springs

ARTICLE INFO

Keywords:

Malware Classification
long short-term memory (LSTM)
Opcode
Natural Language Processing (NLP)
API Calls
Convolutional Neural Network

ABSTRACT

In this paper, we propose a novel model for a malware classification system based on Application Programming Interface (API) calls and opcodes, to improve classification accuracy. This system uses a novel design of combined Convolutional Neural Network and Long Short-Term Memory. We extract opcode sequences and API Calls from Windows malware samples for classification. We transform these features into N-grams (N = 2, 3, and 10)-gram sequences. Our experiments on a dataset of 9,749,57 samples produce high accuracy of **99.91%** using the 8-gram sequences. Our method significantly improves the malware classification performance when using a wide range of recent deep learning architectures, leading to state-of-the-art performance. In particular, we experiment with ConvNeXt-T, ConvNeXt-S, RegNetY-4GF, RegNetY-8GF, RegNetY-12GF, EfficientNetV2, Sequencer2D-L, Swin-T, ViT-G/14, ViT-Ti, ViT-S, ViT-B, ViT-L, and MaxViT-B. Among these architectures, Swin-T and Sequencer2D-L architectures achieved high accuracies of 99.82% and 99.70%, respectively, comparable to our CNN-LSTM architecture although not surpassing it.

1. Introduction

Malware is malicious code that enters a computer or an internet-connected device to steal sensitive information from government, commercial or private organizations. Internet-connected devices infected with malware can also destroy and/or gain access to confidential information, randomly reboot, track user activity, make devices run slower, start unknown processes, or send emails without user action. Classifying malware is complicated because most malware developers adopt strategies to avoid anti-virus systems. Therefore, it is important to fight common and modern evasion techniques to improve the analysis results. Reverse engineering helps understand how a malware works by monitoring runtime execution using dynamic analysis tools, giving insightful information.

Reverse engineering is the process of analyzing software in order to understand its design, functionality, and behavior. This technique is often used in malware analysis to identify and understand the nature of malicious code. Some examples of how reverse engineering is used in malware analysis are given below.

- **Disassembling code:** One of the primary techniques used in reverse engineering is disassembling the code of a malware sample. This process involves converting the binary code of the malware into human-readable assembly language, which can then be analyzed to understand the behavior of the malware.
- **Malware Analysis:** Another important technique in reverse engineering is malware analysis, which involves running the malware in a controlled en-

vironment and analyzing its behavior as it executes. This can help identify the specific functions and routines used by the malware, as well as any malicious behavior it exhibits.

- **Developing countermeasures:** Reverse engineering can also be used to develop countermeasures to malware. By analyzing the code of a malware sample, researchers can identify its specific characteristics and develop tools and techniques to detect and remove it from infected systems.

Overall, reverse engineering is an important technique in malware analysis, helping researchers understand the behavior of malicious code and develop effective countermeasures to protect against it. In January 2023, researchers discovered that malware authors had begun using VSCode malware extensions as a new attack vector to launch malicious attacks. These extensions can take many forms, such as adware, spyware, or even ransomware. Reverse engineering techniques can be used to analyze the code of these extensions in order to understand their behavior and develop effective countermeasures¹. Malware authors have created a new Rootkit malware that harbors JavaScript code that, when launched, paves the way for additional payloads such as SNOW-CONE Cobalt Strike, FONELAUNCH, and Beacon².

Additionally, Application Programming Interfaces (API) allow different software applications or systems to communicate and interact with each other. Malware can exploit API vulnerabilities to execute unauthorized actions, manipulate data, or gain access to sensitive information. An opcode is a part of the machine code, which is a low-level representation of instructions that a computer processor can execute. Malware often uses specific sequences of opcodes to carry out malicious

*Corresponding author: Tel.: +1-970-581-6683;

✉ abensaou@uccs.edu (A. Bensaoud); jkalita@uccs.edu (J. Kalita)

Kalita

ORCID(s):

¹<https://www.esecurityplanet.com/threats/vscode-security>

²<https://thehackernews.com/2023/01/gootkit-malware-continues-to-evolve.html>

activities, such as gaining unauthorized access, stealing sensitive information, or spreading further within a system. Advanced machine learning algorithms can be used to analyze massive amounts of API call data and establish baseline behaviors for normal API interactions. Machine learning models can then be trained to detect deviations from these baselines, helping identify and prevent malware attacks. They can be trained to recognize opcode patterns that are indicative of malware. By analyzing large datasets of opcode sequences, these algorithms can learn to detect new and emerging threats that may not have known signatures.

Over the last few years, researchers have developed various approaches to classify malware using text (code) or images. Recently, methods from computer vision, machine learning, deep learning, and transfer learning have been used to detect malware automatically [1, 2, 3, 4]. In particular, Deep learning is used as a feature extractor that enhances classification accuracy [5].

Transfer learning can be effective for malware image classification tasks. Transfer learning involves taking a deep learning model that has been pre-trained on a large dataset of non-malware images (malware files in binary 2-D format arranged in a matrix like an image) and fine-tuning it on a smaller dataset of malware images. By doing so, the model can learn to classify malware images with high accuracy without requiring as much labeled data. One approach to employing transfer learning for malware image classification involves using a pre-trained convolutional neural network (CNN) as a feature extractor. The CNN is trained on a large dataset of non-malware images, and its weights are frozen. The malware images are then passed through the CNN to obtain feature vectors, which are then used to train a classifier. The classifier can be a simple linear classifier or a more complex model, such as a support vector machine (SVM) or a random forest. Another approach is to **fine-tune** the entire pre-trained CNN on the malware images. This involves unfreezing some or all of the layers of the pre-trained CNN and training them on the malware images while also updating the weights of the classifier. This approach can be more effective than using the pre-trained CNN as a feature extractor since the entire model can be optimized for the malware classification task.

Additionally, exploiting Application Programming Interface (API) vulnerabilities and analyzing opcodes (machine code instructions) offer insights into malware behavior. Advanced machine learning algorithms, particularly those employing deep learning architectures, have proven effective in analyzing massive datasets of API calls and opcode sequences to detect and prevent malware attacks.

Our paper introduces a novel approach to classify malware, focusing on opcode sequences and API calls extracted from diverse malware samples. The main contributions of this paper include:

- **Innovative Classification Model:** We propose a novel model for classifying malware families, in-

corporating Convolutional Neural Network (CNN), Long Short-Term Memory (LSTM), and techniques inspired by Natural Language Processing (NLP). This innovative model aims to enhance classification accuracy. In addition, our approach to representing API calls and opcode sequences is novel, further improving the results.

- **Empirical Evaluation:** We conduct extensive experiments to assess the performance of various fine-tuned recent pre-trained deep learning models, including ConvNeXt-T [6], ConvNeXt-S [6], RegNetY-4GF[7], RegNetY-8GF[7], RegNetY-12GF[7], EfficientNetV2 [8], Sequencer2D-L [9], ViT-G/14 [10], ViT-Ti [11], ViT-S [11], ViT-B [12], ViT-L [12], Max ViT-B [13], and Swin-T [14]. Our evaluations provide empirical evidence of the effectiveness of our proposed CNN-LSTM approach with innovative representation for API calls and opcode sequences, showcasing advancements in malware classification.

Both contributions collectively aim to advance the field of malware classification by introducing innovative approach, providing empirical evidence of effectiveness and highlighting how our approach compares with a large number of very recent methods. The remainder of this paper is organized as follows: Section 2 discusses related work, Section 3 details feature extraction techniques, Section 4 explains the methodologies, Section 5 presents the dataset, Section 6 details the experiments and results, Section 7 provides a short analysis, and the paper concludes with Section 8, which includes the references. All notations used in the paper are listed in Table 13.

2. Related work

In the realm of malware classification, the combination of Convolutional Neural Networks (CNNs) and Long Short-Term Memory (LSTM) networks has emerged as a powerful strategy. CNNs excel in extracting latent features from non-sequential data, particularly images, while LSTMs are adept at capturing dependencies within sequential data, making them invaluable for classification and prediction tasks. The proposition of a CNN-LSTM model for malware classification stems from the synergistic advantages these models offer. CNNs contribute by filtering noise and extracting crucial features from input data, while LSTMs efficiently capture intricate sequence patterns. This strategic amalgamation exploits the strengths of both deep learning approaches, resulting in a notable enhancement in malware classification performance.

2.1. CNN-LSTM Models for Malware Classification

Zhang [15] introduced a CNN-LSTM framework for malware classification by extracting features from n-grams of API calls. Peng et al. [16] proposed an Attention-Based CNN-LSTM model for detecting malicious URLs,

achieving 98.18% accuracy. Sun et al. [17] developed a CNN-LSTM model for intrusion detection using network traffic data, achieving 98.67% accuracy on the CIDS2017 dataset. Kuang et al. [18] designed Deep-WAF to detect web attacks in HTTP requests using CNN-LSTM. Praanna et al. [19] presented a CNN-LSTM model for intrusion detection, leveraging spatial and temporal features for improved performance.

2.2. Transfer Learning for Malware Classification

García et al. [20] proposed a method to evaluate the effectiveness of transfer learning techniques in malware detection, contributing valuable insights. Chaganti et al. [21] introduced an EfficientNetB1-based malware classification approach, achieving a remarkable 99% accuracy on the Microsoft Malware Classification Challenge (MMCC) dataset with fewer parameters. Khan et al. [22] conducted a comprehensive analysis of older pre-trained models (Inception-V4, ResNet18, ResNet34, ResNet50, ResNet101, ResNet152) for malware classification on the MMCC dataset, and highlighted the superior performance of ResNet152 with a testing accuracy of 88.36%. Ullah et al. [23] employed the Bidirectional Encoder Representations from Transformers (BERT) model [24] for feature extraction, introducing a unique malware-to-image conversion algorithm. They utilized the FAST (Features from Accelerated Segment Test) [25] extractor and BRIEF (Binary Robust Independent Elementary Features) descriptor [26] to efficiently extract and emphasize significant features. The trained and texture features were then combined and balanced using the Synthetic Minority Over-Sampling (SMOTE) [27] method and a CNN network was employed to extract deep features. The study employed a balanced ensemble model, incorporating CNN networks for deep feature extraction, leading to effective malware classification and detection.

This paper not only underscores the significance of CNN-LSTM models in malware classification, but also highlights recent advancements in the integration of transfer learning techniques, demonstrating how to further push the boundaries of efficacy in malware detection.

3. Feature Extraction Techniques

In order to use the transfer learning models as well as a custom CNN-LSTM model we propose, we need to extract features of malware. Two feature extraction techniques, Bag of Words (BoW), and TF-IDF are used. One-hot-encoding is used to represent categorical features.

3.1. Term Frequency-Inverse Document Frequency (TF-IDF)

Term Frequency-Inverse Document Frequency (TF-IDF) is a statistical measure used to evaluate the importance of a word in a document. It is commonly used in

text mining and information retrieval.

The formula for TF-IDF is:

$$TF-IDF(t, d) = tf(t, d) \cdot idf(t). \quad (1)$$

In equation 1, $tf(t, d)$ is the frequency of term t in document d , $idf(t)$ is the inverse document frequency of term t across all documents in the corpus. In particular, the term frequency $tf(t, d)$ is the number of times term t appears in document d . In our case, a document is the text of the code in an API and opcodes as well. The inverse document frequency $idf(t)$ is calculated as:

$$idf(t) = \log \frac{N}{df(t)}. \quad (2)$$

In equation 2, N is the total number of documents in the corpus, and $df(t)$ is the number of documents in the corpus that contain term t . Logarithmic scaling is used to prevent the bias towards the commonly occurring terms. TF-IDF gives higher weight to terms that appear frequently in a particular document, but are rare across all documents. The total number of documents refers to the total number of malware samples in our dataset.

3.2. Bag of Words (BoW)

A bag of words represents the frequency of occurrence of each unique word within a document, without considering semantic or grammatical knowledge. BoW involves representing malware samples as a collection of unique words or features extracted from their code or associated metadata. BoW can also be used for the construction of feature vectors for deep learning algorithms.

3.3. Concatenation of BoW and TF-IDF

We simply concatenate TF-IDF features and BoW features for malware as shown in Figure 1.

3.4. N-Gram Representation

The n-gram representation keeps the count of various sequences of n opcodes/API calls. We can represent malware features based on the idea of n-grams. We can set different n -values ($n = 1, 2, \dots, N$) to run various experiments. Experiments are conducted with $n = 2..10$.

3.5. One-Hot Encoding

One-Hot Encoding is a technique used to transform categorical features into numeric that can be used for machine learning algorithms. This technique counts the unique values and assigns a unique index to each value.

3.6. API Collection and Opcode

We extract the API calls and opcodes using two virtual environments, Postman³ and SoapUI⁴. The goals

³<https://www.postman.com>

⁴<https://www.soapui.org>

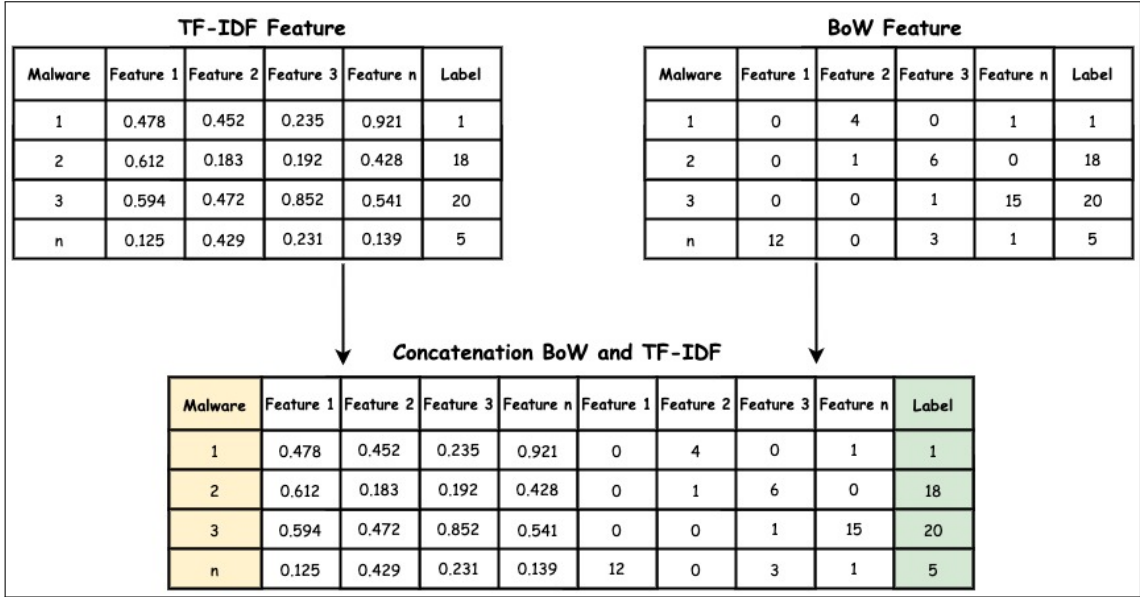


Figure 1: Obtain TF-IDF and BoW for each malware sample and then concatenate.

for using these tools are to extract Native APIs such as low-level APIs or undocumented APIs, thus going beyond regular APIs and get an extensive number of features. All Native APIs begin with the "Zw" or "Nt" prefixes, e.g., NtRemoveProcessDebug and ZwCreateFile.

3.7. Transfer learning

Transfer learning (TL) uses a model that has been pre-trained on one task with a lot of data that can be fine-tuned and used for a different task that does not have a lot of data to train. We evaluate the transfer learning capabilities of various CNN and Transformer architectures and compare the accuracy of classification of the malware dataset. This research uses fourteen recent pre-trained models: ConvNeXt-T [6], ConvNeXt-S [6], RegNetY-4GF [7], RegNetY-8GF [7], RegNetY-12GF [7], EfficientNetV2 [8], Sequencer2D-L [9], ViT-G/14 [10], ViT-Ti [11], ViT-S [11], ViT-B [12], ViT-L [12], MaxViT-B [13], and Swin-T [14] for malware classification. By transferring the knowledge from these models, even with limited labeled data, one can still achieve good classification performance on malware data. All these models offer a practical and effective solution for classification tasks by leveraging pre-trained models' learned representations, reducing training time and resource requirements, and improving generalization and robustness on limited labeled data.

3.7.1. Vision Transformers (ViTs)

Vision Transformers (ViTs) have achieved state-of-the-art image classification performance using self-attention. ViTs utilize the Transformer architecture for computer vision tasks. ViTs [28, 29, 30] show excellent results on the ImageNet classification. The Vision Transformer has developed rapidly in recent years, with a number of variants such as ViT-Ti, ViT-S, ViT-B, ViT-L, Swin-T, MaxViT-B to the recent ViT-G/14.

ViT-Ti [11], **ViT-S** [11], **ViT-B** [12], and **ViT-L** [12] based Transformers incorporate self-attention on patch-level information to perform better feature extraction.

The **Swin-T** [14] Transformer is composed of an even number of Transformer blocks that replace the standard multi-head self-attention module (MSA) with a shifted-window multi-head self-attention (SW-MSA) and window multi-head self-attention (W-MSA). Swin-T aims to solve problems of computational complexity and lack of information interaction between groups of Transformer layers. Swin-T consists of four stages, where each stage reduces the resolution of the input feature map to expand the approachable field layer by layer. Swin-T can automatically learn from an n-dimensional data matrix and find discriminative and representative features and obtain final classification results.

The Transformer learns global features, but lacks inductive bias and often overfits the training set, unlike CNN, which learns inductive bias but does not learn global features [31]. However, **MaxViT-B** can learn local features at the same time as learning global features [13].

3.7.2. ConvNeXt-T & ConvNeXt-S

ConvNeXt was proposed by Facebook AI Research (FAIR) and UC Berkeley in 2022. ConvNeXt-T [6] and ConvNeXt-S [6] are variations of the ConvNeXt CNN architecture. ConvNeXt-T is a smaller and lighter version, suitable for resource-constrained environments, while ConvNeXt-S provides a balance between model size and performance. Both models leverage grouped convolutions to efficiently capture spatial and channel relationships, making them effective choices for various classification tasks.

3.7.3. *RegNetY-4GF & RegNetY-8GF & RegNetY-12GF*

The RegNet [7] type models impose a restriction that there is a linear parameterization of block widths, where the block is a modular unit based on the standard residual bottleneck block with group convolution:

$$u_j = w_0 + w_\alpha \cdot j. \quad (3)$$

In equation 3, u_j represents the width of the block at index j within the range $j < d$, where d represents the depth of the network. The parameter $w_0 > 0$ signifies a base width for the block, while $w_\alpha > 0$ determines the slope of the linear relationship, influencing the width increases with the depth index j . RegNetX [7] has an additional restriction which sets the bottleneck ratio $b = 1$, $12 \leq d \leq 28$ and $w_m \geq 2$, where w_m is the width multiplier. RegNetY [7] is a fast network that uses residual bottlenecks with a group of simple convolutional models that use the Squeeze-and-Excitation [32] operation. Squeeze-and-Excitation improves the strength of a network by explicitly modeling the interdependencies between the channels of its convolutional features.

3.7.4. *EfficientNetV2*

EfficientNetV2 [8] is a family of convolutional neural network architectures designed to achieve high performance while being computationally efficient. It is an evolution of the original EfficientNet [33] models and introduces several improvements and advancements. EfficientNetV2 incorporates a compound scaling method that uniformly scales up the network's depth, width, and resolution to achieve better accuracy. It also introduces a new model scaling technique called "CoDA" (Compound Domain Adaptation) [34] that further enhances performance across different domains.

3.7.5. *Sequencer2D-L*

The Sequencer2D-L [9] model uses LSTMs rather than self-attention layers where the LSTMs are arranged as vertical and horizontal LSTMs to enhance performance. The specific architectural details and optimizations of Sequencer2D-L may vary, but the overarching idea revolves around utilizing LSTMs to effectively transfer learned representations from pre-training tasks to new sequential data in a transfer learning setting.

4. Methodology

This study proposes a CNN-LSTM model, in addition to fine-tuning of the state-of-the-art transfer learning models discussed above for modern malware classification. We compare results produced by these classifiers.

In our feature engineering strategy, we discovered that the use of 8-gram feature vectors for API calls and opcodes produces an effective integration of advanced techniques. Specifically, we employ natural language processing methods such as bag-of-words (BOW), Term

Frequency-Inverse Document Frequency (TF-IDF), and One-hot Encoding as discussed in Subsections 3.1-3.5. These techniques are carefully chosen to capture the diverse nuances of data characteristics, with each method contributing to enhance the representation of the dataset.

The resultant feature vectors, identified as X and Y, serve crucial roles in strengthening our model's discernment capabilities. X, generated through the One-hot Encoding of n-grams, produces a feature vector that clearly outlines the presence of specific sequences of API calls within the dataset. Concurrently, Y takes shape as a feature vector resulting from the intentional concatenation of BOW and TF-IDF representations of grams, giving a richer representation on individual API calls in context.

This purposeful fusion combines the simplicity of BOW with the nuanced representational capability derived from TF-IDF's weighted approach, fostering a comprehensive understanding of the data. The interplay of X and Y within our model not only ensures a holistic grasp of intricate patterns, but also elevates the adaptability and sophistication of our CNN-LSTM architecture and our fine-tuned transfer learning architectures, positioning them as effective solutions for landscape of malware classification. This refined feature engineering methodology, with its incorporation of diverse representations, underscores our model's ability to address the complexity of malware classification, offering a robust and versatile solution.

To convert the concatenated representation to an n-dimensional space, let us denote the Bag-of-Words (BoW) representation as $\text{BoW}(f)$ for a file f containing API calls and opcodes, and the Term Frequency-Inverse Document Frequency (TF-IDF) representation as $\text{TFIDF}(f)$, which also contains API calls and opcodes. The data come from 8-grams, and we convert the concatenated representation to an n-dimensional space by concatenating BoW and TF-IDF representations for each file as follows:

$$\text{Concatenated}(f)_n = [\text{BoW}(f)_1, \text{BoW}(f)_2, \dots, \text{BoW}(f)_C, \text{TFIDF}(f)_1, \text{TFIDF}(f)_2, \dots, \text{TFIDF}(f)_C]$$

$$X = \text{Concatenated}(f)_n$$

where C is the size of the opcode and API call. We assume n is the dimensionality of the concatenated feature vector. This is shown in Figure 1.

Additionally, we introduce a new feature Y where Y is constructed as a One-Hot Encoding from the 8-grams. This means that for each 8-gram in the dataset, Y will have a binary entry indicating its presence or absence in a particular malware file.

4.1. Custom CNN-LSTM Model

The CNN-LSTM model is designed to effectively classify malware families based on the abstraction and representation of 8-gram sequences involving API calls and opcodes. The model employs a combination of Convolutional Neural Network (CNN) and Long Short-

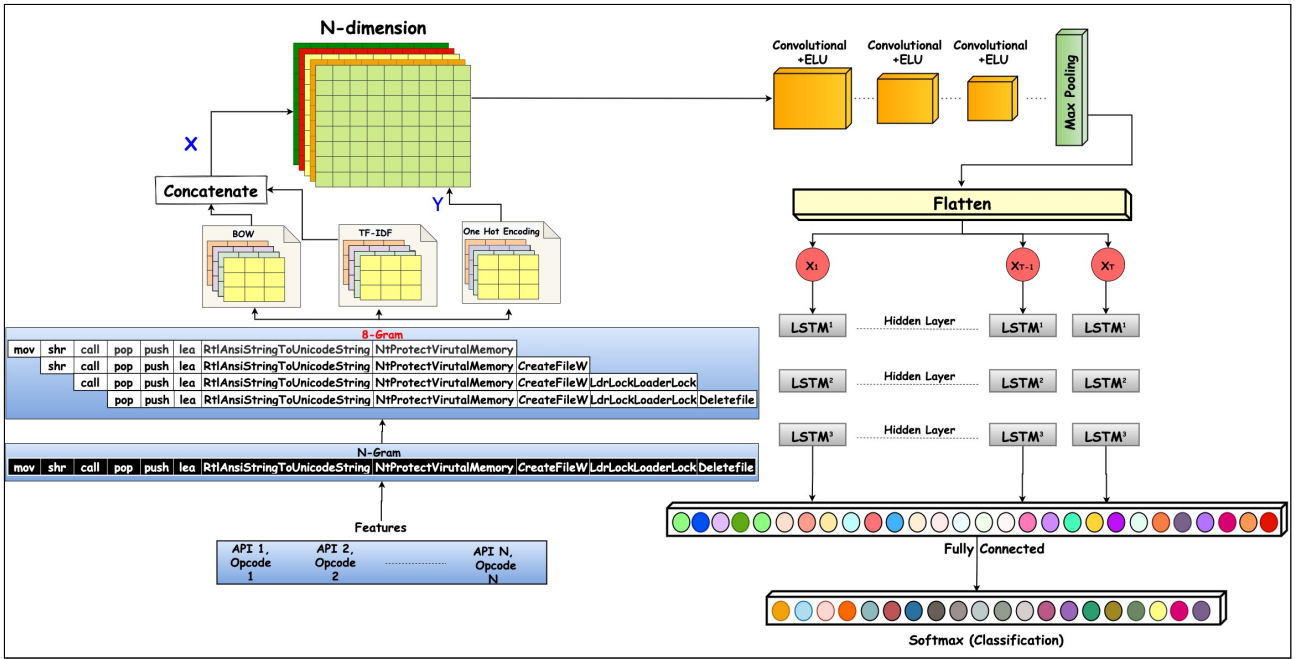


Figure 2: Proposed model of CNN-LSTM.

Term Memory (LSTM) networks to automate the generation of sequential feature maps for this specific malware classification task.

The CNN was used to extract complex features from the 8-dimensional matrix, and LSTM was used for classification. The model has three convolutional layers, three pooling layers, three LSTM layers, one fully connected layer. The size of the convolutional layer used for feature extraction is 9×9 . We use the ELU activation function [35]. Max-pooling kernels of size 3×3 are used to reduce the dimensions of the feature maps. Subsequently, a flatten layer is used to transform the output into a one-dimensional vector. At the end of the CNN, the feature map is transferred to the LSTM layer. The model architecture includes an LSTM layer with 512 neurons, a depth of 3, and a dropout rate of 0.3. This LSTM component enhances the model’s capacity to discern intricate patterns within the sequential data. The proposed architecture that mixes two deep learning models is shown in Figure 2.

The optimization process for the model involved 200 epochs and a batch size of 64 during training. The Adam optimizer, featuring a learning rate of 0.001, was preferred for its adaptive learning rate calculations, making it a suitable choice for efficient optimization. This combination of architectural intricacies with especially constructed features, underscores the model’s robustness and effectiveness in malware classification. The pseudocode for CNN-LSTM-3 is given in Algorithm 1.

In our experimentation, we compared GRU, LSTM, RNN, and CNN models with the proposed hybrid CNN-LSTM-3 architecture for malware classification, utilizing opcodes and API calls as input features. The objective was to thoroughly assess and compare the per-

formance of the proposed model against a number of recent high-performing CNN models.

4.2. Fine-tuned State-of-the-art Models

In second proposed approach, we adopted the same input structure that was used in the previous model and applied it to various transfer learning models, as shown in Figure 3.

Fine-tuning is a crucial component of the transfer learning approach, allowing for reuse of a selection of pre-trained layers to enhance overall performance. In our endeavor to improve the accuracy of pre-trained models, we implemented specific fine-tuning configurations. The models discussed earlier in Section 3.7 have been fine-tuned for the classification of 20 malware families.

All models are fine-tuned by adjusting the pre-trained weights to suit the specific task.

Let θ denote the parameters of a pre-trained model, and \mathcal{L} represent the loss function used for training. The standard objective is to minimize this loss as shown in equation 4:

$$\text{Fine-tuning objective: } \underset{\theta}{\text{minimize}} \mathcal{L}(\theta). \quad (4)$$

During fine-tuning, the model is typically trained on a new dataset related to the malware families. Let \mathcal{D}_{new} represent this dataset, and \mathcal{L}_{new} denote the corresponding loss function as illustrated in equation 5:

$$\mathcal{L}_{\text{new}}(\theta) = \frac{1}{|\mathcal{D}_{\text{new}}|} \sum_{(x,y) \in \mathcal{D}_{\text{new}}} \mathcal{L}(\theta, x, y). \quad (5)$$

Fine-tuning involves updating the weights (θ) based on the gradients of the loss with respect to the parameters,

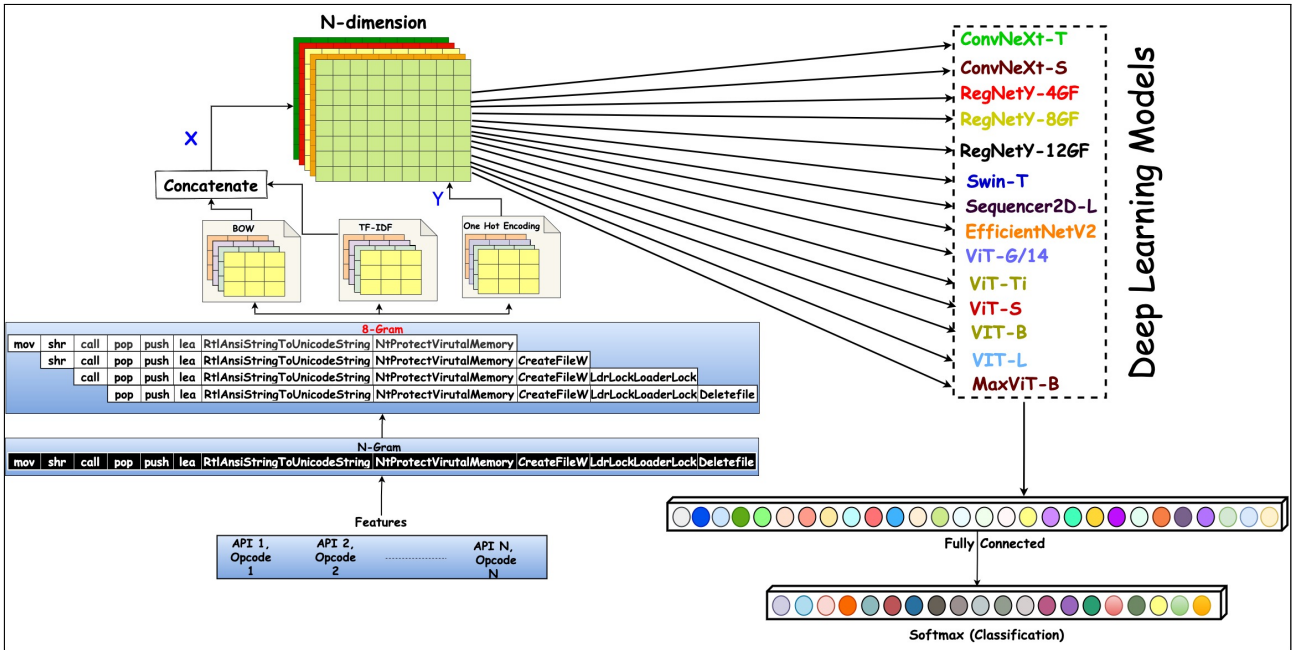


Figure 3: Proposed approach with deep learning models compared.

as outlined in equation 6:

$$\theta \leftarrow \theta - \alpha \nabla_{\theta} \mathcal{L}_{\text{new}}(\theta). \quad (6)$$

Here, α is the learning rate.

In EfficientNetV2, Swin-T, and Sequencer2D-L, we froze all pre-trained layers from the utilized architectures. Subsequently, we replaced the final fully connected (FC) layers, originally designed for the ImageNet dataset, with our custom FC layers. In the case of RegNetY-4GF, RegNetY-8GF, and RegNetY-12GF, we customized the heads of the models and added GlobalAveragePooling2D and Dense layers to the end of each model.

We customized ViT-G/14, ViT-Ti, ViT-S, ViT-B, ViT-L, and MaxViT-B by placing a linear layer on top of pre-trained ViT models where the linear layer is positioned on top of the last hidden state of the class CLS token, which serves as a robust representation of the entire input. We also customized the number of output neurons. We obtained saved parameter checkpoints for the ViT models as detailed in [28]. Algorithm 2 shows the pseudocode for training various modern fine-tuned pre-trained models.

5. Dataset

We created a dataset of 9,749,57 different malware examples and 89,004 benign examples. All malware samples were collected from VirusShare and VirusTotal between 2019 to 2023 while all benign samples collected between 2021 to 2023⁵; See Table 1.

⁵<https://github.com/abensaou-uccs/API-calls-and-opcodes-malware-dataset>

Table 1

The most dangerous malware families

Family name	Number of samples
WanaCrypt0r	70001
Ryuk	91205
MicroCop	40048
Xorist	54307
CobraLocker	20081
Sodinokibi	15000
Banload	40401
Dialer	32206
Aimbot	49019
Rbot	18002
SpyBot	20011
StartPage	32126
Mytob	86988
Banker	15415
Limr	73451
Hupigon	60704
Agobot	84091
Dyfuca	97563
IstBar	74338
Benign	89004

6. Experiments and Results

We performed a series of experiments to test the efficacy of fourteen pre-training models and the custom CNN-LSTM model. All experiments were repeated seven times and the accuracy was calculated by averaging the results from all seven runs.

6.1. Experiment #1: CNN-LSTM Models

We designed four LSTM models with different configurations as shown in Table 2.

Algorithm 1 CNN-LSTM-3 for Malware Classification

```
1:   n = 8                                     ▷ Choose the value of n between 0 and 11 for n-grams
2:   function NGRAMSEXTRACT(file, n)
3:     grams ← []
4:     for j from 0 to length(file) - n do     ▷ Compute n-grams and store in files
5:       ngram ← substring(file, j, j + n)
6:       grams.append(ngram)
7:     return grams
8:   Construct a TF-IDF model from grams
9:   Construct a BoW model from grams
10:  y ← Construct a OneHotEncoding from grams
11:  x ← Concatenate BoW and TF-IDF
12:  n-dimension ← x and y
13:  _____
14:  Input n-dimension
15:  Convolutional layers with Exponential Linear Unit ELU activation:
16:    Conv2D(NumFilters, KernelSize, Stride, Padding)
17:    ELU Activation
18:    MaxPooling
19:  Flatten layer
20:  LSTM Layer 1 with NumHiddenUnits hidden units
21:  LSTM Layer 2 with NumHiddenUnits hidden units
22:  LSTM Layer 3 with NumHiddenUnits hidden units
23:  Fully connected layers:
24:    Output layer with softmax activation: Dense(NumClasses=20, activation='softmax')
25:  Train the model on input n-dimension and labels
26:  Evaluate the model's performance
27:  Make classification on new n-dimension
```

Table 2
LSTM configurations of different sizes.

Hyper parameters	LSTM-1	LSTM-2	LSTM-3	LSTM-4
Number of neurons	128	256	512	1024
Weight for updating algorithm	Adam	Adam	Adam	Adam
Window size	150	250	200	250
Depth	1	2	3	4
Epoch	200	200	200	200
Dropout rate	0.2	0.3	0.3	0.3
Batch size	32	64	64	64

Table 3 shows the performance measures for malware classification using our collected dataset. The precision, recall, and F1-score values are given for 20 malware classes shown in table 1. The CNN-LSTM-3 model outperformed the others, with a classification rate of 99.91%. CNN-LSTM-3 performed well for malware classification, while GRU, RNN, and CNN did not have ideal results. Overall, the CNN-LSTM-3 model delivered the best classification for malware classification in terms of precision, recall, and F1 score. The proposed CNN-LSTM-3 model achieved 0.01, 99.84, 99.91, 99.99, and 99.87, Average Accuracy, Precision, Recall, and F1-score, respectively, which are the best rates when compared to Sequence-to-Sequence GRU and RNN models, and CNN model. As shown in Figure 4, the error rate of the training process of CNN-LSTM-3 is significantly lower than the other models. The results pre-

sented in Figure 5 show the high accuracy and efficiency of the hybrid CNN-LSTM-3 method.

6.2. Experiment #2: State-of-the-Art Pre-trained Models

All pre-trained models were fine-tuned on our dataset.

The **ViT-G/14** model was fine-tuned using AdamW [36] with $\beta_1 = 0.8$ and $\beta_2 = 0.8$ and weight decay of 0.1. We fine-tuned the three pre-trained regulated residual **RegNet** [7] architectures of different capacities, **RegNetY-4GF** [7], **RegNetY-8GF** [7], and **RegNetY-12GF** [7] and **ConvNeXt-T** [6] and **ConvNeXt-S** [6] on our dataset; See Table 4. For **Swin-T** configuration, see Table 5. In Swin-T, we froze the parameters for the first three stages and we used the AdamW optimizer. In **EfficientNetV2**, we froze the layers of EfficientNetV2 with the weights of ImageNet, and added

Algorithm 2 Modern Fine-tuned Transfer Learning Models for Malware Classification

```
1:   n = 8                                     ▷ Choose the value of n between 0 and 11 for n-grams
2:   function NGRAMSEXTRACT(file, n)
3:     grams ← []
4:     for j from 0 to length(file) - n do
5:       ngram ← substring(file, j, j + n)
6:       grams.append(ngram)
7:     return grams
8: Construct a TF-IDF model from grams
9: Construct a BoW model from grams
10: y ← Construct a OneHotEncoding from grams
11: x ← Concatenate BoW and TF-IDF
12: n-dimension ← x and y
13: _____
14: Input n-dimension
15:
16: switch Model do
17:   case 1: ConvNeXt-T                       ▷ Initializing a model from the ConvNeXt-T style configuration.
18:
19:   case 2: ConvNeXt-S                       ▷ Initializing a model from the ConvNeXt-S style configuration.
20:
21:   case 3: RegNetY-4GF                     ▷ Initializing a model from the RegNetY-4GF style configuration.
22:
23:   case 4: RegNetY-8GF                     ▷ Initializing a model from the RegNetY-8GF style configuration.
24:
25:   case 5: RegNetY-12GF                   ▷ Initializing a model from the RegNetY-12GF style configuration.
26:
27:   case 6: EfficientNetV2                 ▷ Initializing a model from the EfficientNetV2 style configuration.
28:
29:   case 7: Sequencer2D-L                 ▷ Initializing a model from the Sequencer2D-L style configuration.
30:
31:   case 8: ViT-G/14                       ▷ Initializing a model from the ViT-G/14 style configuration.
32:
33:   case 9: ViT-Ti                         ▷ Initializing a model from the ViT-Ti style configuration.
34:
35:   case 10: ViT-S                         ▷ Initializing a model from the ViT-S style configuration.
36:
37:   case 11: ViT-B                         ▷ Initializing a model from the ViT-B style configuration.
38:
39:   case 12: ViT-L                         ▷ Initializing a model from the ViT-L style configuration.
40:
41:   case 13: MaxViT-B                      ▷ Initializing a model from the MaxViT-B style configuration.
42:
43:   case 14: Swin-T                       ▷ Initializing a model from the Swin-T style configuration.
44:
45: Fully connected layers:
46:   Output layer with softmax activation: Dense(NumClasses=20, activation='softmax')
47: Train the model on input n-dimension and labels
48: Evaluate the model's performance
49: Make classification on new n-dimension
```

extra dense layers to facilitate the classification of 20 classes. See EfficientNetV2 configuration in Table 6.

For Sequencer2D-L, we use base learning rate $\frac{batchsize}{512} \times 5 \times 10^{-4}$ where batch size is 2048. Sequencer2D-L achieves results that are competitive with Swin-T. For ViT-G/14, ViT-Ti, ViT-S, ViT-B, ViT-L, and MaxViT-

B; we fine-tuned only the multi-head attention layers and froze the feedforward network (FFN) layers to reduce the memory peak during training. The pre-trained ViT models get results with drastically different performances. In Table 7, we make a comparison among these state-of-the-art pre-trained models in terms of accuracy. Table 8 shows the comparison of the perfor-

Table 3
Comparative accuracy of CNN classifiers with LSTM models and other classifiers.

Models	Loss	Max Acc (%)	Min Acc (%)	Average Acc (%)	Precision (%)	Recall (%)	F1-score (%)
GRU	1.49	89.99	80.42	89.29	88.90	88.65	88.12
RNN	2.13	85.65	83.59	84.72	86.43	82.39	85.70
CNN	1.20	90.71	88.52	89.12	90.27	89.57	90.36
CNN-LSTM-1	0.091	92.54	90.29	90.82	91.11	90.41	90.30
CNN-LSTM-2	0.081	91.30	90.63	90.99	91.43	92.22	92.89
CNN-LSTM-3	0.0014	99.98	99.90	99.91	99.88	99.89	99.87
CNN-LSTM-4	0.18	91.81	89.73	90.44	91.67	90.63	90.72

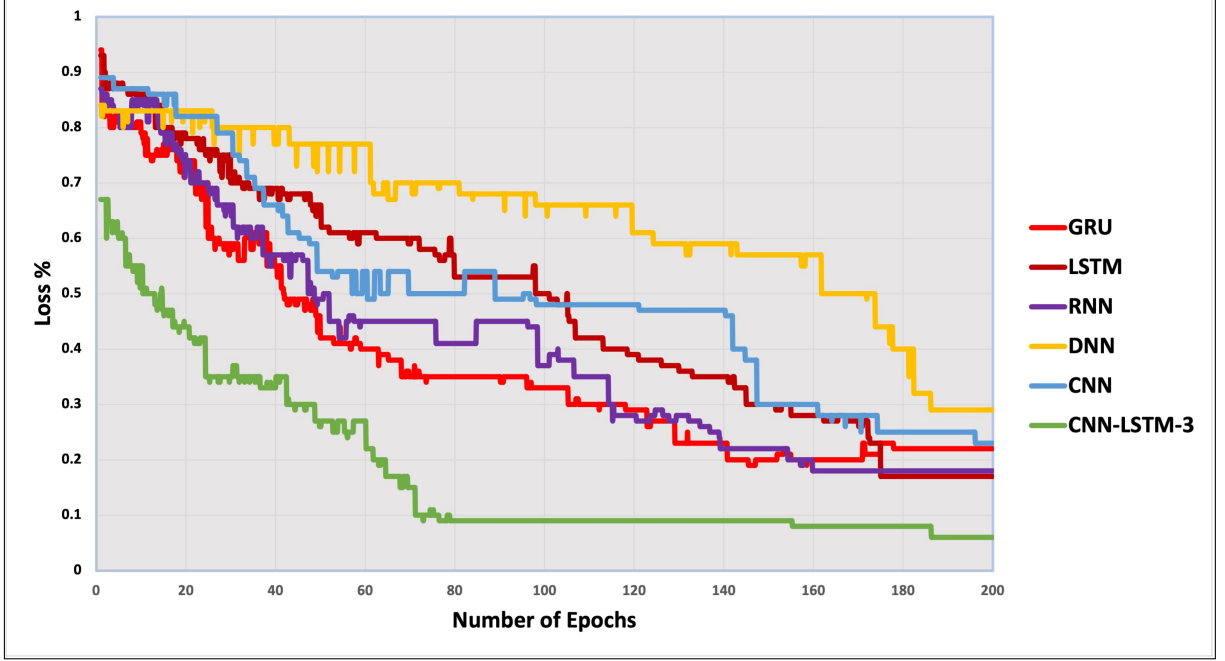


Figure 4: Loss trends for various deep learning models. Clearly, the CNN-LSTM-3 model has the lowest loss all through as the number of epochs increases.

mance among state-of-the-art models for malware sequences classification. Figure 6 illustrates the efficient training speed of our model CNN-LSTM-3 compared to other models. We use confusion matrices to visualize classification performance. As an example, the confusion matrix of transfer learning for CNN-LSTM-3 is presented in Figure 7. The final experimental results show that Sequencer2D-L and Swin-T effectively classify malware families in our dataset.

In Table 9, which shows classification accuracy for different N-gram models, it is evident that the 8-gram model consistently outperforms other N-gram configurations. Across various transfer learning models, including CNN-LSTM, the 8-gram model consistently achieves high accuracy results. These findings justify the use of the 8-gram model for enhanced accuracy and reliability in classification tasks.

6.3. Evaluation Metrics

We used Accuracy, Recall, Precision, and F1-score metrics to evaluate the models for malware detection. Equation 7 defines Accuracy, which measures the over-

all correctness of predictions as shown below:

$$Accuracy = \frac{TP + TN}{TP + TN + FP + FN}. \quad (7)$$

In equation 8, Precision measures the accuracy of positive predictions among the instances predicted as positive:

$$Precision = \frac{TP}{TP + FP}. \quad (8)$$

Equation 9, referring to Recall, quantifies the ability to identify all relevant instances in the dataset:

$$Recall = \frac{TP}{TP + FN}. \quad (9)$$

Equation 10, defines the F1-score, which balances Precision and Recall to provide a single metric for model evaluation:

$$F1 = \frac{2 * Precision * Recall}{Precision + Recall} = \frac{2 * TP}{2 * TP + FP + FN}. \quad (10)$$

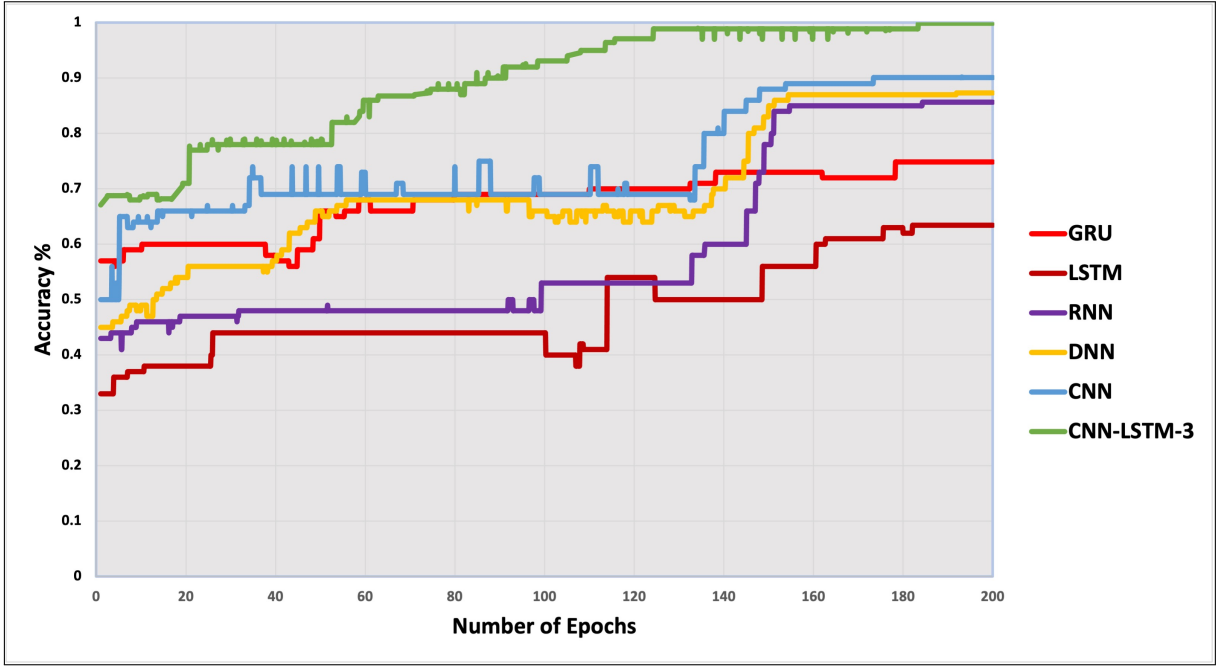


Figure 5: Accuracy trends for various deep learning models. The CNN-LSTM-3 model has the best accuracy as the number of epochs increases.

Table 4

Fine-tuning configurations for RegNetY-4GF, RegNetY-8GF, RegNetY-12GF, ConvNeXt-T and ConvNeXt-S networks.

Pre-Training Model	Optimizer	Weight Decay	Learning Rate Schedule	Weight Init	Optimizer Momentum	Layer Scale	CutMix	Warmup Schedule
ConvNeXt-T	Adam	0.01	cosine decay	Truncated Normal(0.2)	$\beta_1 = 0.5$ $\beta_2 = 0.5$	1e+06	1.0	2e+5
ConvNeXt-S	Adam	0.01	cosine decay	Truncated Normal(0.2)	$\beta_1 = 0.6$ $\beta_2 = 0.6$	1e+06	1.0	2e+5
RegNetY-4GF	Adam	0.05	cosine decay	Gaussian distribution $\mathcal{N}(0, 0.01)$	$\beta_1 = 0.5$ $\beta_2 = 0.9$	0.0001	-	0.06
RegNetY-8GF	Adam	0.05	cosine decay	Gaussian distribution $\mathcal{N}(0, 0.01)$	$\beta_1 = 0.6$ $\beta_2 = 0.8$	0.0001	-	0.05
RegNetY-12GF	Adam	0.05	cosine decay	Gaussian distribution $\mathcal{N}(0, 0.01)$	$\beta_1 = 0.6$ $\beta_2 = 0.7$	0.0001	-	0.07

In these formulas, TP is true positive, FP is false positive, TN is true negative, and FN is false negative. In the confusion matrix, the misclassification numbers below the off-diagonal are categorized as FNs, and the number of misclassifications above the off-diagonal are considered FPs. The TNs are the numbers of correctly classified examples for other classes than the actual class.

7. Discussion

Fine-tuning pre-trained Swin-T and Sequencer2D-L models achieve higher accuracy and improve convergence speed. Currently, only Swin-T and Sequencer2D-L have only been pre-trained using a malware dataset, and our experiments have demonstrated enough transferability when applied straight to other malware families. We believe that pre-trained Swin-T and Sequencer2D-

Table 5

Fine-tuning configuration of Swin-T network.

Pre-Training Model	Initializer Range	Layer Norm Eps	Window Size	Number of MLP	Depths	Number of Heads	Encoder Stride
Swin-T	0.2	1e+06	16	1024	[2, 2, 6, 2]	[2, 6, 12, 24]	32

Table 6
Fine-tuning configuration of EfficientNetV2 network.

Pre-Training Model	Decay	Momentum	Weight Decay
EfficientNets	0.7	0.90	1e+5

Table 7
Classification accuracy on our dataset.

Model	Family	Number of Parameter	Optimizer	batch size	Training epochs	Max Acc	Min Acc	Avg Acc
ConvNeXt-T [6]	CNN	29 Milion	Adam [37]	512	300	87.06	82.43	85.30
ConvNeXt-S [6]	CNN	50 Milion	Adam [37]	512	200	89.94	86.37	87.21
RegNetY-4GF [7]	CNN	21 Milion	RMSProp [38]	512	100	92.76	90.81	91.16
RegNetY-8GF [7]	CNN	39 Milion	RMSProp [38]	512	100	91.82	88.02	90.82
RegNetY-12GF [7]	CNN	46 Milion	RMSProp [38]	512	100	92.33	85.81	89.07
EfficientNetV2 [8]	CNN	24 Milion	RMSProp [38]	512	200	92.38	88.15	90.54
Sequencer2D-L [9]	Sequences	54 Milion	AdamW [36]	2048	300	99.73	99.66	99.70
ViT-G/14 [10]	Transformer	600 Milion	Adam [37]	1024	200	94.20	90.50	93.12
ViT-Ti [11]	Transformer	5.8 Milion	Adam [37]	1024	200	92.48	90.45	91.72
ViT-S [11]	Transformer	22.2 Milion	Adam [37]	1024	200	89.67	84.31	88.49
VIT-B [12]	Transformer	86 Milion	Adam [37]	1024	200	90.55	89.16	90.04
VIT-L [12]	Transformer	307 Milion	Adam [37]	1024	200	90.23	87.59	89.60
MaxViT-B [13]	Transformer	119 Milion	Adam [37]	1024	200	88.65	81.41	85.07
Swin-T [14]	Transformer	28 Milion	AdamW[36]	1024	200	99.94	99.79	99.82

L models can benefit from transfer learning to perform various malware image analysis tasks, such as classification and detection.

The confusion matrices for the ConvNeXt-T, ConvNeXt-S, RegNetY-4GF, RegNetY-8GF, RegNetY-12GF, EfficientNetV2, ViT-G/14, ViT-Ti, ViT-S, VIT-B, VIT-L and MaxViT-B models show that some malware varieties are still classified incorrectly, which reflects the need to improve further the ability of the models to extract sufficient features so that they can provide better performance in terms of the metrics. **By comparing the performance of different models, we find that**

the proposed CNN-LSTM-3 is better than even the Swin-T and Sequencer2D-L models in terms of performance and classification.

We evaluated the performance of fifteen models using Analysis-of-Variance (ANOVA) [39]. Table 10 shows the ANOVA results in the form of F-statistics and p-values for each model. The ANOVA summary provides valuable insights into the comparative analysis of these models. Notably, CNN-LSTM-3 demonstrated exceptional accuracy at 99.91%, making it a standout performer. Conversely, models like ConvNeXt-T and MaxViT-B showed comparatively lower accuracy per-

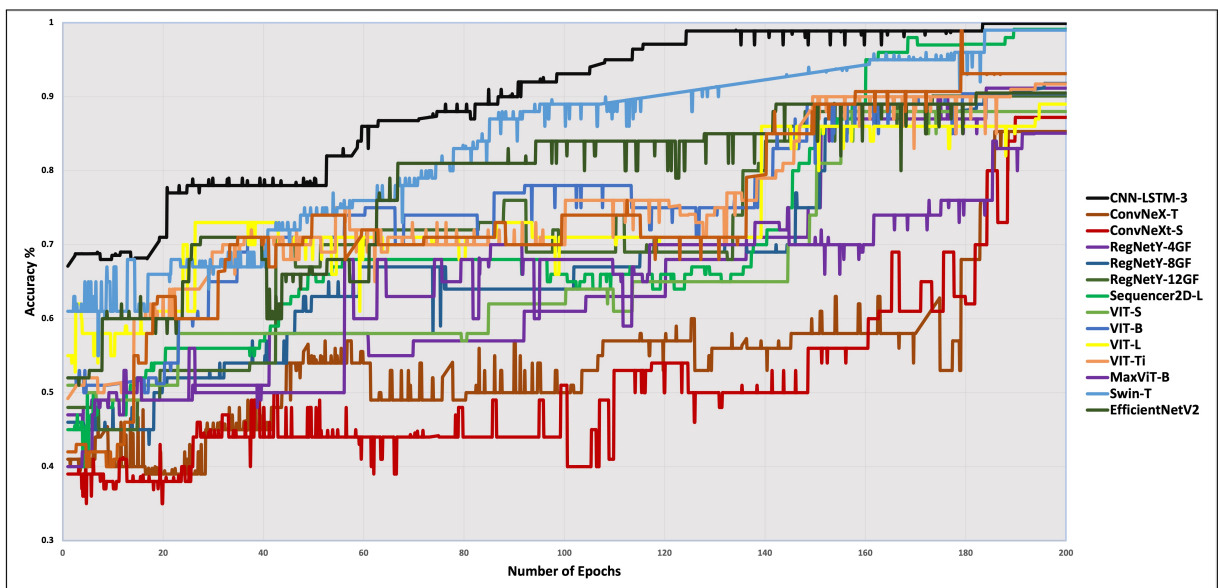


Figure 6: Plot the accuracy vs. epoch for all models. The consistently lowest model is MaxViT-B, while the consistently highest model is CNN-LSTM-3.

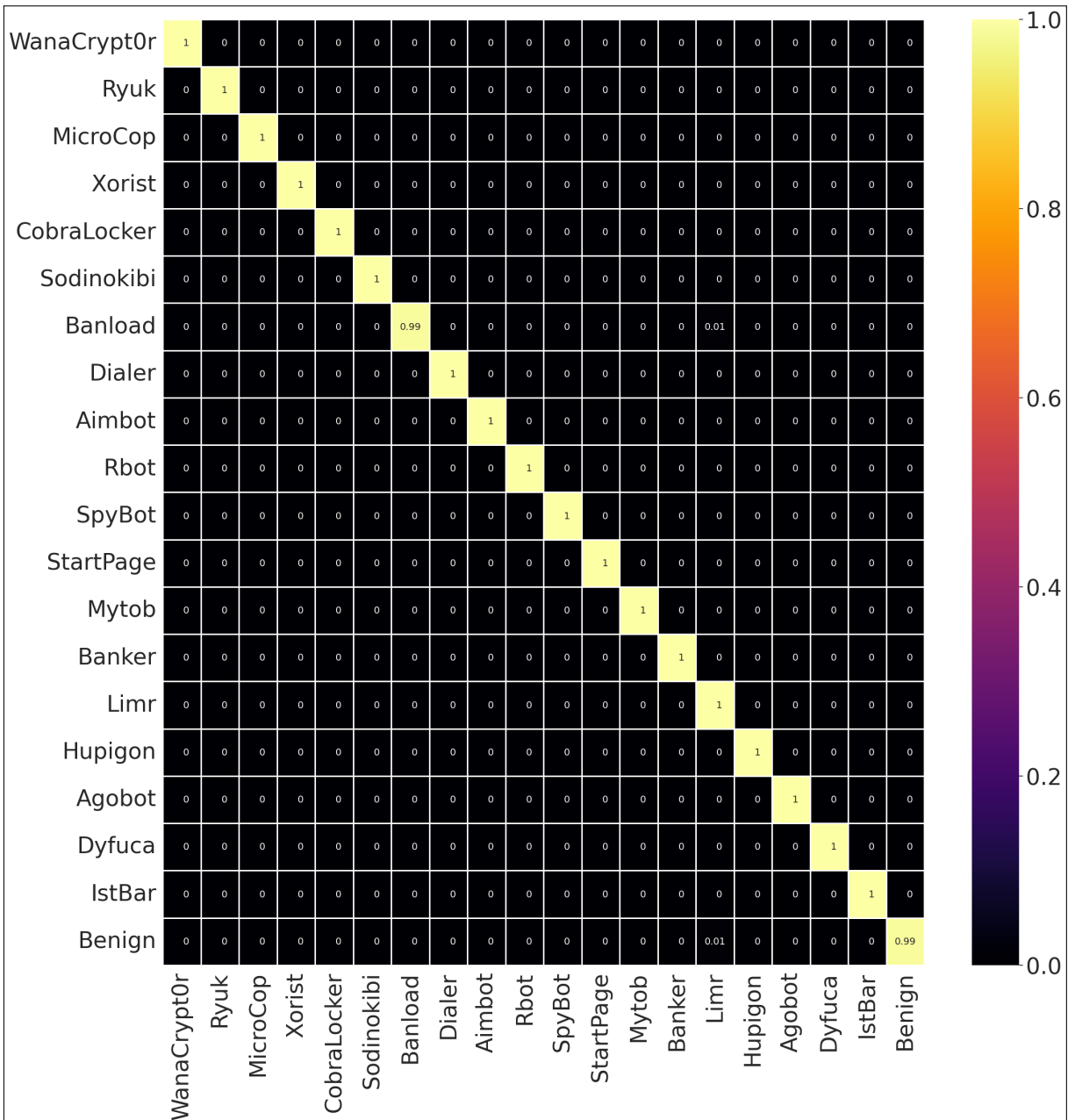


Figure 7: Confusion matrix for CNN-LSTM-3 malware classification. Confusion matrices are generated for each classification experiment. This one is provided as an example.

centages at 85.30% and 85.07%, respectively. The ANOVA results, represented through F-statistics and p-values, offer statistical significance for each model’s performance across the tasks. For instance, models such as CNN-LSTM-3, Sequencer2D-L, and Swin-T exhibited significantly superior performance, as indicated by their low p-values ($p < 0.01$). In contrast, models like ConvNeXT-T and MaxViT-B did not show statistically significant differences in their accuracy scores across tasks, as suggested by their p-values ($p > 0.05$).

The F values and p values represent important statistical measures for the analysis performed. For example, $F1$ indicates that the F-statistic is calculated for the first model (CNN-LSTM-3). It measures the ratio of variance between the accuracy scores of CNN-LSTM-

3 across different tasks to the variance within the accuracy scores of CNN-LSTM-3 within those tasks. Additionally, 14 represents the degrees of freedom associated with the numerator of the F-statistic. In ANOVA, degrees of freedom refer to the number of values in the final calculation of a statistic that are free to vary. In this case, there are 15 models, so there are $15 - 1 = 14$ degrees of freedom for the numerator. Moreover, the p-values (e.g., $p = 0.002$, $p = 0.325$, etc.) indicate the level of significance for each F-statistic. Lower p-values imply higher statistical significance, indicating that the differences in accuracy scores among the models are unlikely to be due to random variation. In addition, Table 11 shows the performance metrics and the best results are denoted in bold.

Table 8

Result based comparison between our model and other state-of-the-art models that used different datasets. These results are collected from published papers. Even though the results are not directly comparable, they are given here for completeness as recommended by reviewers.

Model	Number of malicious files	Classes	Accuracy	Type
LSTM [2020]	7107	8	95%	API Calls
Gradient Classifier [2019]	39000	-	94.64%	API Calls
CNN-bidirectional LSTM [2020]	15931	-	96.76%	API Calls
CNN [2019]	174607	-	98.82%	API Calls
BiLSTM [2023]	-	-	93.16%	API Calls
TextCNN [2020]	-	-	95.90%	API Calls
RNN [2020]	20,000	-	91%	API Calls
BERT [2021]	5000	4	96.76%	API Calls
Our model CNN-LSTM-3	9,749,57	20	99.91%	API Calls and opcodes

Based on the provided ANOVA table, CNN-LSTM-3 demonstrates the highest level of statistical significance among the models Sequencer2D-L and Swin-T as shown in Figure 8. The p-value associated with CNN-LSTM-3 ($p = 0.002$) is considerably lower than the p-values of both Sequencer2D-L ($p = 0.007$) and Swin-T ($p = 0.005$). A lower p-value indicates higher statistical significance, suggesting that the observed differences in accuracy scores for CNN-LSTM-3 are less likely to be due to random variation compared to Sequencer2D-L and Swin-T. Therefore, according to the ANOVA analysis, CNN-LSTM-3 is the most statistically significant model among these three when comparing their performance across different tasks.

In analyzing the results presented in the table 12, it is evident that the CNN-LSTM-3 model consistently outperforms both Sequencer2D-L and Swin-T across multiple publicly available datasets of malware samples. Specifically, CNN-LSTM-3 achieves an impressive accuracy of 99.89% on the VirusSamples dataset, 99.89% on MalShare, 99.90% on VirusTotal, 99.90% on Dynamite AI Lab, and 99.88% on the Zoo GitHub. In comparison, Sequencer2D-L and Swin-T, while commendable with 98.52% and 98.87% accuracy rates, respectively on certain datasets, fall behind CNN-LSTM-3. This substantial margin suggests that CNN-LSTM-3 exhibits a superior capability to discern patterns within malware samples using API calls and opcode information. Its robust performance underscores its potential as a preferred model for accurate and reliable malware detection, making it a promising choice.

8. CONCLUSIONS

We designed a novel CNN-LSTM architecture and use techniques from Natural Language Processing for classifying both known malware and unknown malware families. Using Postman and SoapUI virtual environments, we extracted not only regular API calls, but also native API calls and opcodes. We extracted 8-grams from API calls and opcodes to compute TF-IDF, BoW, and one-hot encoding and converted them to n -dimensional matrices. We compared GRU, LSTM, RNN, and CNN

with our model. Experimental results demonstrate that our model achieved the best performance, reaching an accuracy of 99.91% with statistical significance. Our work is one of the first attempts to fine-tune Vision Transformers (ViTs) for malware classification. A comparison of all pre-trained models performed revealed that, while ConvNeXt-T, ConvNeXt-S, RegNetY-4GF, RegNetY-8GF, RegNetY-12GF, EfficientNetV2, ViT-G/14, ViT-Ti, ViT-B, ViT-S, ViT-L, and MaxViT-B performed well, the Swin-T and Sequencer2D-L Transformer outperformed all the state-of-the-art models in terms of accuracy, providing an accuracy of 99.83% and 99.70% respectively. Our experiments demonstrate that although many of the state-of-the-art CNN and Transformer-based models are excellent in malware classification, a simpler CNN-LSTM model performs equally well, if not better.

References

- [1] A. Bensaoud, N. Abudawaood, J. Kalita, Classifying malware images with convolutional neural network models, *International Journal of Network Security* 22 (2020) 1022–1031.
- [2] S. Yoo, S. Kim, S. Kim, B. B. Kang, Ai-hydra: Advanced hybrid approach using random forest and deep learning for malware classification, *Information Sciences* 546 (2021) 420–435.
- [3] Ö. Aslan, A. A. Yilmaz, A new malware classification framework based on deep learning algorithms, *Ieee Access* 9 (2021) 87936–87951.
- [4] Z. He, A. Rezaei, H. Homayoun, H. Sayadi, Deep neural network and transfer learning for accurate hardware-based zero-day malware detection, in: *Proceedings of the Great Lakes Symposium on VLSI 2022*, 2022, pp. 27–32.
- [5] M. Dib, S. Torabi, E. Bou-Harb, C. Assi, A multi-dimensional deep learning framework for iot malware classification and family attribution, *IEEE Transactions on Network and Service Management* 18 (2021) 1165–1177.
- [6] Z. Liu, H. Mao, C.-Y. Wu, C. Feichtenhofer, T. Darrell, S. Xie, A convnet for the 2020s, in: *Proceedings of the IEEE/CVF Conference on Computer Vision and Pattern Recognition*, 2022, pp. 11976–11986.
- [7] I. Radosavovic, R. P. Kosaraju, R. Girshick, K. He, P. Dollár, Designing network design spaces, in: *Proceedings of the IEEE/CVF conference on computer vision and pattern recognition*, 2020, pp. 10428–10436.
- [8] Z. Leng, M. Tan, C. Liu, E. D. Cubuk, X. Shi, S. Cheng, D. Anguelov, Polyloss: A polynomial expansion perspective of

Table 9
Classification accuracy using different N-gram features.

N-gram	N									
	1	2	3	4	5	6	7	8	9	10
CNN-LSTM-3	62.25%	69.89%	74.35%	72.98%	70.21%	68.93%	77.75%	99.91%	69.89%	57.49%
ConvNeXt-T [6]	31.87%	30.18%	32.54%	30.19%	31.50%	32.69%	31.44%	85.30%	35.81%	32.89%
ConvNeXt-S [6]	60.22%	61.41%	60.92%	61.57%	60.10%	66.31%	62.54%	87.21%	73.17%	60.14%
RegNetY-4GF [7]	40.76%	52.93%	43.01%	60.21%	58.28%	64.53%	70.30%	91.16%	69.48%	50.11%
RegNetY-8GF [7]	62.67%	56.23%	65.10%	69.87%	60.97%	57.85%	67.29%	90.82%	63.04%	66.56%
RegNetY-12GF [7]	61.90%	56.66%	47.77%	68.39%	54.42%	57.11%	48.26%	89.07%	44.79%	63.55%
EfficientNetV2 [8]	45.58%	53.28%	71.72%	57.26%	63.23%	49.83%	62.97%	90.54%	54.82%	61.76%
Sequencer2D-L [9]	48.09%	52.42%	56.23%	60.83%	74.22%	65.46%	80.66%	99.70%	78.65%	76.03%
ViT-G/14 [10]	50.46%	64.96%	65.64%	72.04%	74.79%	79.14%	70.87%	93.12%	77.43%	79.98%
ViT-Ti [11]	51.18%	53.63%	76.34%	64.79%	70.00%	72.64%	66.47%	91.72%	72.06%	68.74%
ViT-S [11]	52.75%	63.47%	67.98%	50.95%	56.93%	62.29%	79.55%	88.49%	71.07%	62.60%
VIT-B [12]	55.74%	63.60%	75.09%	68.20%	69.19%	75.72%	80.01%	90.04%	81.21%	65.09%
VIT-L [12]	48.49%	60.45%	56.44%	63.69%	49.99%	79.27%	75.08%	89.60%	68.07%	50.15%
MaxViT-B [13]	50.90%	47.73%	65.97%	48.57%	51.66%	48.70%	65.13%	85.07%	76.00%	72.55%
Swin-T [14]	60.91%	78.74%	44.90%	78.18%	77.98%	78.23%	71.53%	99.82%	75.04%	69.16%

Table 10
ANOVA summary for fifteen classification models.

Model	Accuracy (%)	ANOVA Summary
CNN-LSTM-3	99.91	F1,14 = 3.45, p = 0.002
ConvNeXt-T	85.30	F2,14 = 1.12, p = 0.325
ConvNeXt-S	87.21	F3,14 = 1.78, p = 0.112
RegNetY-4GF	91.16	F4,14 = 2.67, p = 0.018
RegNetY-8GF	90.82	F5,14 = 2.45, p = 0.027
RegNetY-12GF	89.07	F6,14 = 2.12, p = 0.055
EfficientNetV2	90.54	F7,14 = 2.31, p = 0.035
Sequencer2D-L	99.70	F8,14 = 3.11, p = 0.007
ViT-G/14	93.12	F9,14 = 2.85, p = 0.012
ViT-Ti	91.72	F10,14 = 2.74, p = 0.015
ViT-S	88.49	F11,14 = 2.05, p = 0.071
VIT-B	90.04	F12,14 = 2.21, p = 0.049
VIT-L	89.60	F13,14 = 2.18, p = 0.052
MaxViT-B	85.07	F14,14 = 1.97, p = 0.065
Swin-T	99.82	F15,14 = 3.31, p = 0.005

Table 11
Classification performance for fifteen classification models with Accuracy, Precision, Recall, F1 Score, and AUC Score.

Model	Accuracy (%)	Precision (%)	Recall (%)	F1 Score (%)	AUC Score
CNN-LSTM-3	99.91	99.62	99.62	99.62	99.62
ConvNeXt-T	85.30	80.10	80.10	80.10	80.10
ConvNeXt-S	87.21	84.79	84.79	84.79	84.79
RegNetY-4GF	91.16	87.82	87.82	87.82	87.82
RegNetY-8GF	90.82	87.31	87.31	87.31	87.31
RegNetY-12GF	89.07	88.45	88.45	88.45	88.45
EfficientNetV2	90.54	89.11	89.11	89.11	89.11
Sequencer2D-L	99.70	96.39	96.39	96.39	96.39
ViT-G/14	93.12	91.83	91.83	91.83	91.83
ViT-Ti	91.72	90.24	90.24	90.24	90.24
ViT-S	88.49	84.06	84.06	84.06	84.06
VIT-B	90.04	89.70	89.70	89.70	89.70
VIT-L	89.60	85.53	85.53	85.53	85.53
MaxViT-B	85.07	81.92	81.92	81.92	81.92
Swin-T	99.82	97.14	97.14	97.14	97.14

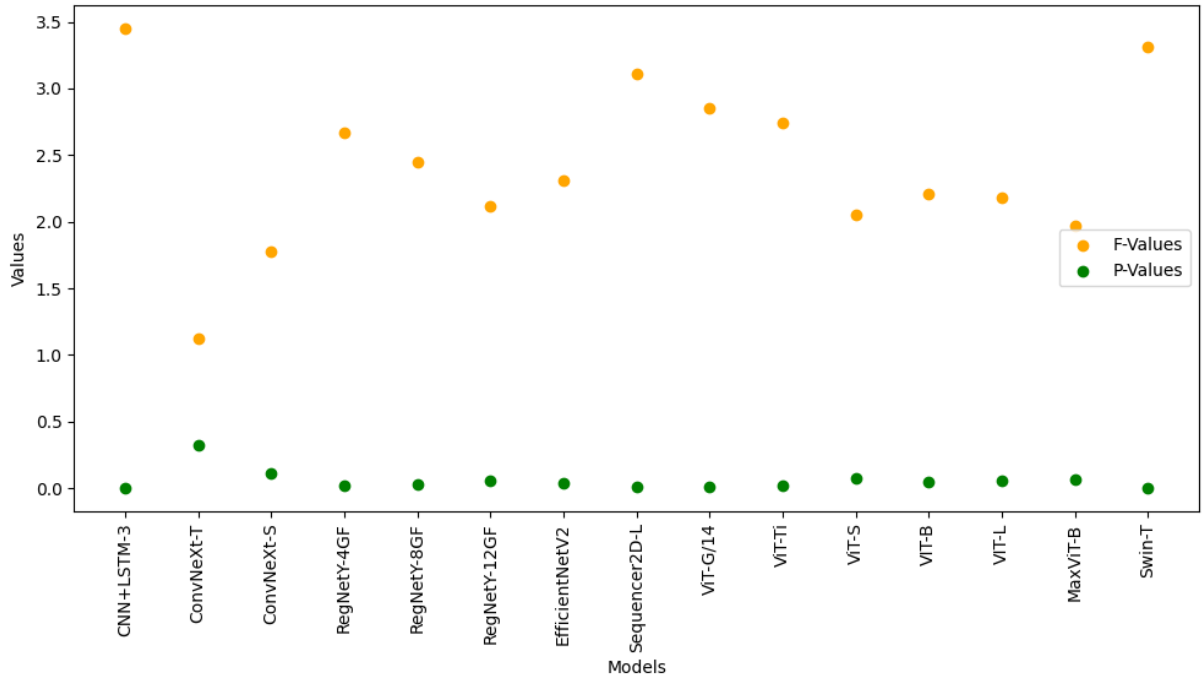


Figure 8: ANOVA test results for the fifteen different models.

Table 12

Testing stat-of-the-art CNN and Transformer-based and our high perform CNN-LSTM-3 models on publicly available datasets containing malware samples with API calls and opcode information.

Model	VirusSamples	MalShare	VirusTotal	Dynamite AI Lab	The Zoo GitHub
CNN-LSTM-3	99.89%	99.89%	99.90%	99.90%	99.88%
ConvNeXt-T	82.43%	82.76%	82.59%	82.10%	82.28%
ConvNeXt-S	83.15%	83.39%	83.94%	83.63%	83.76%
RegNetY-4GF	90.84%	90.22%	90.51%	90.38%	90.61%
RegNetY-8GF	89.27%	89.59%	89.28%	89.55%	89.93%
RegNetY-12GF	85.03%	85.41%	85.35%	85.81%	85.45%
EfficientNetV2	89.70%	89.50%	89.46%	89.06%	89.19%
Sequencer2D-L	98.52%	98.16%	98.09%	98.23%	98.00%
ViT-G/14	90.73%	90.73%	90.73%	90.73%	90.73%
ViT-Ti	89.12%	89.62%	89.33%	89.49%	89.67%
ViT-S	84.81%	84.32%	84.95%	84.77%	84.41%
ViT-B	89.30%	89.83%	89.98%	89.62%	89.36%
ViT-L	85.81%	85.45%	85.93%	85.33%	85.81%
MaxViT-B	80.42%	80.95%	80.07%	80.11%	80.24%
Swin-T	98.87%	98.42%	98.27%	98.13%	98.87%

classification loss functions, arXiv preprint arXiv:2204.12511 (2022).

[9] Y. Tatsunami, M. Taki, Sequencer: Deep lstm for image classification, arXiv preprint arXiv:2205.01972 (2022).

[10] M. Wortsman, G. Ilharco, S. Y. Gadre, R. Roelofs, R. Gontijo-Lopes, A. S. Morcos, H. Namkoong, A. Farhadi, Y. Carmon, S. Kornblith, et al., Model soups: averaging weights of multiple fine-tuned models improves accuracy without increasing inference time, in: International Conference on Machine Learning, PMLR, 2022, pp. 23965–23998.

[11] R. Strudel, R. Garcia, I. Laptev, C. Schmid, Segmenter: Transformer for semantic segmentation, in: Proceedings of the IEEE/CVF international conference on computer vision, 2021, pp. 7262–7272.

[12] M. Dehghani, A. Arnab, L. Beyr, A. Vaswani, Y. Tay, The efficiency misnomer, arXiv preprint arXiv:2110.12894 (2021).

[13] Z. Tu, H. Talebi, H. Zhang, F. Yang, P. Milanfar, A. Bovik, Y. Li, Maxvit: Multi-axis vision transformer, in: Computer Vision–ECCV 2022: 17th European Conference, Tel Aviv, Israel, October 23–27, 2022, Proceedings, Part XXIV, Springer, 2022, pp. 459–479.

[14] Z. Liu, Y. Lin, Y. Cao, H. Hu, Y. Wei, Z. Zhang, S. Lin, B. Guo, Swin transformer: Hierarchical vision transformer using shifted windows, in: Proceedings of the IEEE/CVF international conference on computer vision, 2021, pp. 10012–10022.

[15] J. Zhang, Deepmal: A cnn-lstm model for malware detection based on dynamic semantic behaviours, in: 2020 International Conference on Computer Information and Big Data Applications (CIBDA), 2020, pp. 313–316. doi:10.1109/CIBDA50819.2020.00077.

- [16] Y. Peng, S. Tian, L. Yu, Y. Lv, R. Wang, Malicious url recognition and detection using attention-based cnn-lstm, *KSII Transactions on Internet and Information Systems (TIIS)* 13 (2019) 5580–5593.
- [17] P. Sun, P. Liu, Q. Li, C. Liu, X. Lu, R. Hao, J. Chen, DI-ids: Extracting features using cnn-lstm hybrid network for intrusion detection system, *Security and communication networks* 2020 (2020) 1–11.
- [18] X. Kuang, M. Zhang, H. Li, G. Zhao, H. Cao, Z. Wu, X. Wang, Deepwaf: detecting web attacks based on cnn and lstm models, in: *CyberSpace Safety and Security: 11th International Symposium, CSS 2019, Guangzhou, China, December 1–3, 2019, Proceedings, Part II* 11, Springer, 2019, pp. 121–136.
- [19] K. Praanna, S. Sruthi, K. Kalyani, A. S. Tejaswi, A cnn-lstm model for intrusion detection system from high dimensional data, *J. Inf. Comput. Sci* 10 (2020) 1362–1370.
- [20] D. E. García, N. DeCastro-García, A. L. M. Castañeda, An effectiveness analysis of transfer learning for the concept drift problem in malware detection, *Expert Systems with Applications* 212 (2023) 118724.
- [21] R. Chaganti, V. Ravi, T. D. Pham, Image-based malware representation approach with efficientnet convolutional neural networks for effective malware classification, *Journal of Information Security and Applications* 69 (2022) 103306.
- [22] R. U. Khan, X. Zhang, R. Kumar, Analysis of resnet and googlenet models for malware detection, *Journal of Computer Virology and Hacking Techniques* 15 (2019) 29–37.
- [23] F. Ullah, A. Alsirhani, M. M. Alshahrani, A. Alomari, H. Naeem, S. A. Shah, Explainable malware detection system using transformers-based transfer learning and multi-model visual representation, *Sensors* 22 (2022) 6766.
- [24] J. Devlin, M.-W. Chang, K. Lee, K. Toutanova, Bert: Pre-training of deep bidirectional transformers for language understanding, *arXiv preprint arXiv:1810.04805* (2018).
- [25] D. G. Viswanathan, Features from accelerated segment test (fast), in: *Proceedings of the 10th workshop on image analysis for multimedia interactive services*, London, UK, 2009, pp. 6–8.
- [26] M. Calonder, V. Lepetit, C. Strecha, P. Fua, Brief: Binary robust independent elementary features, in: *Computer Vision—ECCV 2010: 11th European Conference on Computer Vision, Heraklion, Crete, Greece, September 5–11, 2010, Proceedings, Part IV* 11, Springer, 2010, pp. 778–792.
- [27] N. V. Chawla, K. W. Bowyer, L. O. Hall, W. P. Kegelmeyer, Smote: synthetic minority over-sampling technique, *Journal of artificial intelligence research* 16 (2002) 321–357.
- [28] A. Dosovitskiy, L. Beyer, A. Kolesnikov, D. Weissenborn, X. Zhai, T. Unterthiner, M. Dehghani, M. Minderer, G. Heigold, S. Gelly, et al., An image is worth 16x16 words: Transformers for image recognition at scale, *arXiv preprint arXiv:2010.11929* (2020).
- [29] H. Touvron, M. Cord, M. Douze, F. Massa, A. Sablayrolles, H. Jégou, Training data-efficient image transformers & distillation through attention, in: *International conference on machine learning*, PMLR, 2021, pp. 10347–10357.
- [30] W. Wang, E. Xie, X. Li, D.-P. Fan, K. Song, D. Liang, T. Lu, P. Luo, L. Shao, Pyramid vision transformer: A versatile backbone for dense prediction without convolutions, in: *Proceedings of the IEEE/CVF international conference on computer vision*, 2021, pp. 568–578.
- [31] K. Han, A. Xiao, E. Wu, J. Guo, C. Xu, Y. Wang, Transformer in transformer, *Advances in Neural Information Processing Systems* 34 (2021) 15908–15919.
- [32] J. Hu, L. Shen, G. Sun, Squeeze-and-excitation networks, in: *Proceedings of the IEEE conference on computer vision and pattern recognition*, 2018, pp. 7132–7141.
- [33] M. Tan, Q. Le, Efficientnet: Rethinking model scaling for convolutional neural networks, in: *International conference on machine learning*, PMLR, 2019, pp. 6105–6114.
- [34] M. Chen, Z. Xu, K. Weinberger, F. Sha, Marginalized denoising autoencoders for domain adaptation, *arXiv preprint arXiv:1206.4683* (2012).
- [35] D.-A. Clevert, T. Unterthiner, S. Hochreiter, Fast and accurate deep network learning by exponential linear units (elus), *arXiv preprint arXiv:1511.07289* (2015).
- [36] I. Loshchilov, F. Hutter, Decoupled weight decay regularization, *arXiv preprint arXiv:1711.05101* (2017).
- [37] Z. Zhang, Improved adam optimizer for deep neural networks, in: *2018 IEEE/ACM 26th international symposium on quality of service (IWQoS)*, Ieee, 2018, pp. 1–2.
- [38] T. Tieleman, G. Hinton, et al., Lecture 6.5-rmsprop: Divide the gradient by a running average of its recent magnitude, *COURSEREA: Neural networks for machine learning* 4 (2012) 26–31.
- [39] L. St, S. Wold, et al., Analysis of variance (anova), *Chemometrics and intelligent laboratory systems* 6 (1989) 259–272.
- [40] F. O. Catak, A. F. Yazı, O. Elezaj, J. Ahmed, Deep learning based sequential model for malware analysis using windows exe api calls, *PeerJ Computer Science* 6 (2020) e285.
- [41] M. Ijaz, M. H. Durad, M. Ismail, Static and dynamic malware analysis using machine learning, in: *2019 16th International Bhurban Conference on Applied Sciences and Technology (IB-CAST)*, 2019, pp. 687–691. doi:10.1109/IBCAST.2019.8667136.
- [42] Z. Zhang, P. Qi, W. Wang, Dynamic malware analysis with feature engineering and feature learning, in: *Proceedings of the AAAI conference on artificial intelligence*, volume 34, 2020, pp. 1210–1217.
- [43] D. Xue, J. Li, T. Lv, W. Wu, J. Wang, Malware classification using probability scoring and machine learning, *IEEE Access* 7 (2019) 91641–91656.
- [44] C. Avci, B. Tekinerdogan, C. Catal, Analyzing the performance of long short-term memory architectures for malware detection models, *Concurrency and Computation: Practice and Experience* 35 (2023) 1–1.
- [45] B. Qin, Y. Wang, C. Ma, Api call based ransomware dynamic detection approach using textcnn, in: *2020 International Conference on Big Data, Artificial Intelligence and Internet of Things Engineering (ICBAIE)*, IEEE, 2020, pp. 162–166.
- [46] S. Jha, D. Prashar, H. V. Long, D. Taniar, Recurrent neural network for detecting malware, *computers & security* 99 (2020) 102037.
- [47] S. Yesir, İ. Soğukpınar, Malware detection and classification using fasttext and bert, in: *2021 9th International Symposium on Digital Forensics and Security (ISDFS)*, IEEE, 2021, pp. 1–6.

Appendix

Table 13
Mathematical notations for modern transfer learning.

Definition	Notation
Dataset	\mathcal{D}
Model parameters	θ
Loss Function	\mathcal{L}
Dropout rate	γ
Stride	s
Padding	p
Growth rate	Δ
Number of layers	L
Bottleneck ratio	B
Input	x_i
Epsilon term	ϵ
Variance	σ^2
Mean	μ
Width scaling factor	w
Compound scaling coefficient to balance width	w_α
Width multiplier	w_m
Learning rate	η
Optimizer Momentum	β
Number of heads	H_0